CHAPTER

1

RAY OPTICS

Sir Isaac Newton (1642–1727) set forth a theory of optics in which light emissions consist of collections of corpuscles that propagate rectilinearly.

Pierre de Fermat (1601–1665) developed the principle that light travels along the path of least time.

Light is an electromagnetic wave phenomenon described by the same theoretica principles that govern all forms of electromagnetic radiation. Electromagnetic radiatio propagates in the form of two mutually coupled *vector* waves, an electric-field wav and a magnetic-field wave. Nevertheless, it is possible to describe many optica phenomena using a *scalar* wave theory in which light is described by a single scala wavefunction. This approximate way of treating light is called scalar wave optics, o simply **wave optics**.

When light waves propagate through and around objects whose dimensions are much greater than the wavelength, the wave nature of light is not readily discerned, sc that its behavior can be adequately described by rays obeying a set of geometrical rules. This model of light is called **ray optics**. Strictly speaking, ray optics is the limit of wave optics when the wavelength is infinitesimally small.

Thus the electromagnetic theory of light (**electromagnetic optics**) encompasses wave optics, which, in turn, encompasses ray optics, as illustrated in Fig. 1.0-1. Ray optics and wave optics provide approximate models of light which derive their validity from their successes in producing results that approximate those based on rigorous electromagnetic theory.

Although electromagnetic optics provides the most complete treatment of light within the confines of **classical optics**, there are certain optical phenomena that are characteristically quantum mechanical in nature and cannot be explained classically. These phenomena are described by a quantum electromagnetic theory known as **quantum electrodynamics**. For optical phenomena, this theory is also referred to as **quantum optics**.

Historically, optical theory developed roughly in the following sequence: (1) ray optics; → (2) wave optics; → (3) electromagnetic optics; → (4) quantum optics. Not

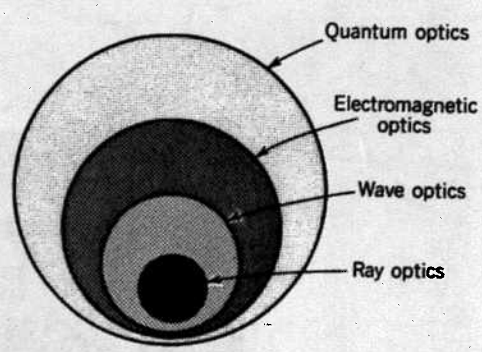

Figure 1.0-1 The theory of quantum optics provides an explanation of virtually all optical phenomena. The electromagnetic theory of light (electromagnetic optics) provides the most complete treatment of light within the confines of classical optics. Wave optics is a scalar approximation of electromagnetic optics. Ray optics is the limit of wave optics when the wavelength is very short.

surprisingly, these models are progressively more difficult and sophisticated, having being developed to provide explanations for the outcomes of successively more complex and precise optical experiments.

For pedagogical reasons, the chapters in this book follow the historical order noted above. Each model of light begins with a set of postulates (provided without proof), from which a large body of results are generated. The postulates of each model are then shown to follow naturally from the next-higher-level model. In this chapter we begin with ray optics.

Ray Optics

Ray optics is the simplest theory of light. Light is described by rays that travel in different optical media in accordance with a set of geometrical rules. Ray optics is therefore also called **geometrical optics**. Ray optics is an approximate theory. Although it adequately describes most of our daily experiences with light, there are many phenomena that ray optics does not adequately describe (as amply attested to by the remaining chapters of this book).

Ray optics is concerned with the *location* and *direction* of light rays. It is therefore useful in studying *image formation*—the collection of rays from each point of an object and their redirection by an optical component onto a corresponding point of an image. Ray optics permits us to determine conditions under which light is guided within a given medium, such as a glass fiber. In isotropic media, optical rays point in the direction of the flow of *optical energy*. Ray bundles can be constructed in which the density of rays is proportional to the density of light energy. When light is generated isotropically from a point source, for example, the energy associated with the rays in a given cone is proportional to the solid angle of the cone. Rays may be traced through an optical system to determine the optical energy crossing a given area.

This chapter begins with a set of postulates from which the simple rules that govern the propagation of light rays through optical media are derived. In Sec. 1.2 these rules are applied to simple optical components such as mirrors and planar or spherical boundaries between different optical media. Ray propagation in inhomogeneous (graded-index) optical media is examined in Sec. 1.3. Graded-index optics is the basis of a technology that has become an important part of modern optics.

Optical components are often centered about an optical axis, around which the rays travel at small inclinations. Such rays are called **paraxial rays**. This assumption is the basis of **paraxial optics**. The change in the position and inclination of a paraxial ray as it travels through an optical system can be efficiently described by the use of a 2×2-matrix algebra. Section 1.4 is devoted to this algebraic tool, called **matrix optics**.

1.1 POSTULATES OF RAY OPTICS

Postulates of Ray Optics

- Light travels in the form of rays. The rays are emitted by light sources and can be observed when they reach an optical detector.
- An optical medium is characterized by a quantity $n \geq 1$, called the **refractive index**. The refractive index is the ratio of the speed of light in free space c_o to that in the medium c. Therefore, the time taken by light to travel a distance d equals $d/c = nd/c_o$. It is thus proportional to the product nd, known as the **optical path length**.

- In an inhomogeneous medium the refractive index $n(\mathbf{r})$ is a function of the position $\mathbf{r} = (x, y, z)$. The optical path length along a given path between two points A and B is therefore

$$\text{Optical path length} = \int_A^B n(\mathbf{r})\, ds,$$

where ds is the differential element of length along the path. The time taken by light to travel from A to B is proportional to the optical path length.

- **Fermat's Principle.** Optical rays traveling between two points, A and B, follow a path such that the time of travel (or the optical path length) between the two points is an extremum relative to neighboring paths. An extremum means that the rate of change is zero, i.e.,

$$\delta \int_A^B n(\mathbf{r})\, ds = 0.$$

The extremum may be a minimum, a maximum, or a point of inflection. It is, however, usually a minimum, in which case

light rays travel along the path of least time.

Sometimes the minimum time is shared by more than one path, which are then all followed simultaneously by the rays.

In this chapter we use the postulates of ray optics to determine the rules governing the propagation of light rays, their reflection and refraction at the boundaries between different media, and their transmission through various optical components. A wealth of results applicable to numerous optical systems are obtained without the need for any other assumptions or rules regarding the nature of light.

Propagation in a Homogeneous Medium

In a homogeneous medium the refractive index is the same everywhere, and so is the speed of light. The path of minimum time, required by Fermat's principle, is therefore also the path of minimum distance. The principle of the *path of minimum distance* is known as **Hero's principle**. The path of minimum distance between two points is a straight line so that *in a homogeneous medium, light rays travel in straight lines* (Fig. 1.1-1).

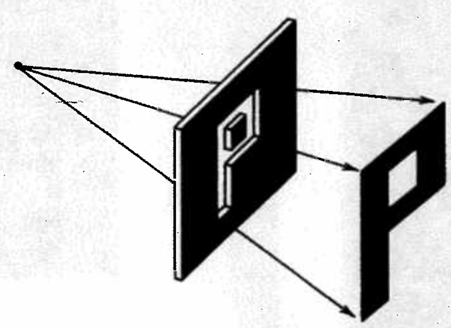

Figure 1.1-1 Light rays travel in straight lines. Shadows are perfect projections of stops.

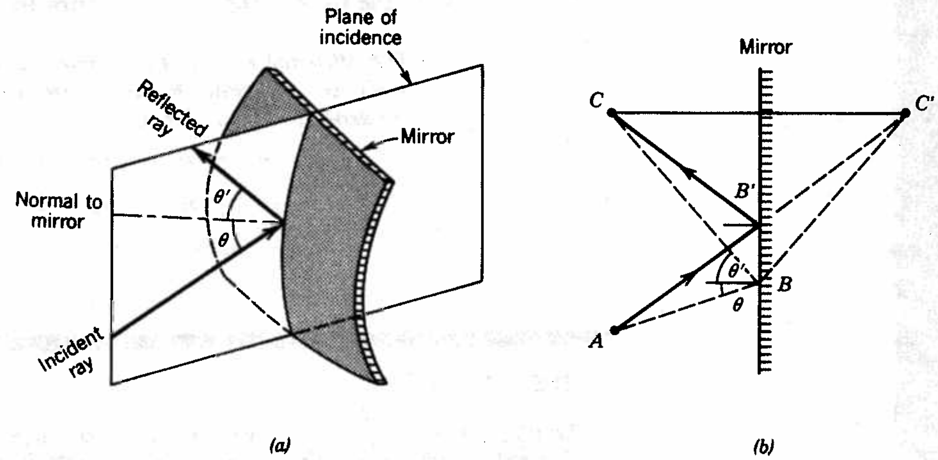

Figure 1.1-2 (*a*) Reflection from the surface of a curved mirror. (*b*) Geometrical construction to prove the law of reflection.

Reflection from a Mirror

Mirrors are made of certain highly polished metallic surfaces, or metallic or dielectric films deposited on a substrate such as glass. Light reflects from mirrors in accordance with the law of reflection:

The reflected ray lies in the plane of incidence;
the angle of reflection equals the angle of incidence.

The plane of incidence is the plane formed by the incident ray and the normal to the mirror at the point of incidence. The angles of incidence and reflection, θ and θ', are defined in Fig. 1.1-2(*a*). To prove the law of reflection we simply use Hero's principle. Examine a ray that travels from point A to point C after reflection from the planar mirror in Fig. 1.1-2(*b*). According to Hero's principle the distance $\overline{AB} + \overline{BC}$ must be minimum. If C' is a mirror image of C, then $\overline{BC} = \overline{BC'}$, so that $\overline{AB} + \overline{BC'}$ must be a minimum. This occurs when $\overline{ABC'}$ is a straight line, i.e., when B coincides with B' and $\theta = \theta'$.

Reflection and Refraction at the Boundary Between Two Media

At the boundary between two media of refractive indices n_1 and n_2 an incident ray is split into two—a reflected ray and a refracted (or transmitted) ray (Fig. 1.1-3). The

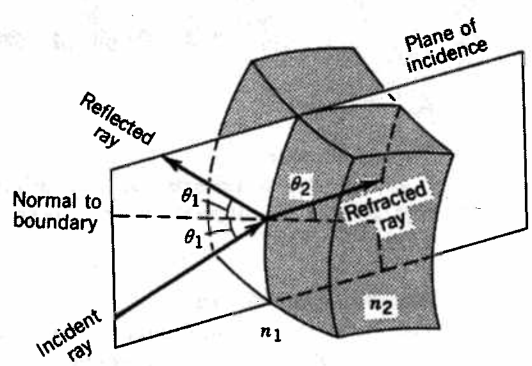

Figure 1.1-3 Reflection and refraction at the boundary between two media.

reflected ray obeys the law of reflection. The refracted ray obeys the law of refraction:

The refracted ray lies in the plane of incidence; the angle of refraction θ_2 is related to the angle of incidence θ_1 by Snell's law,

$$n_1 \sin \theta_1 = n_2 \sin \theta_2. \tag{1.1-1}$$

Snell's Law

EXERCISE 1.1-1

Proof of Snell's Law. The proof of Snell's law is an exercise in the application of Fermat's principle. Referring to Fig. 1.1-4, we seek to minimize the optical path length $n_1\overline{AB} + n_2\overline{BC}$ between points A and C. We therefore have the following optimization problem: Find θ_1 and θ_2 that minimize $n_1 d_1 \sec\theta_1 + n_2 d_2 \sec\theta_2$, subject to the condition $d_1 \tan\theta_1 + d_2 \tan\theta_2 = d$. Show that the solution of this constrained minimization problem yields Snell's law.

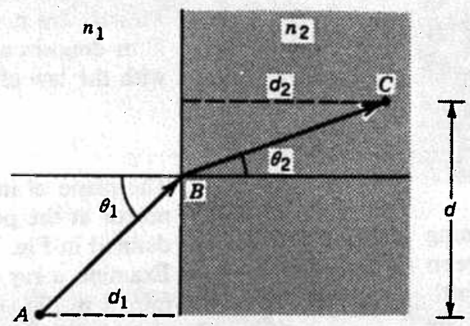

Figure 1.1-4 Construction to prove Snell's law.

The three simple rules—propagation in straight lines and the laws of reflection and refraction—are applied in Sec. 1.2 to several geometrical configurations of mirrors and transparent optical components, without further recourse to Fermat's principle.

1.2 SIMPLE OPTICAL COMPONENTS

A. Mirrors

Planar Mirrors

A planar mirror reflects the rays originating from a point P_1 such that the reflected rays appear to originate from a point P_2 behind the mirror, called the image (Fig. 1.2-1).

Paraboloidal Mirrors

The surface of a paraboloidal mirror is a paraboloid of revolution. It has the useful property of focusing all incident rays parallel to its axis to a single point called the **focus**. The distance $\overline{PF} = f$ defined in Fig. 1.2-2 is called the **focal length**. Paraboloidal law of refraction:

(1.1-1)
Snell's Law

application of
cal path length
ng optimization
to the condition
imization prob-

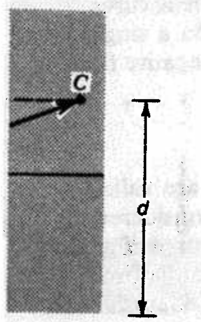

of reflection and
s of mirrors and
principle.

at the reflected
the image (Fig.

t has the useful
point called the
th. Paraboloidal

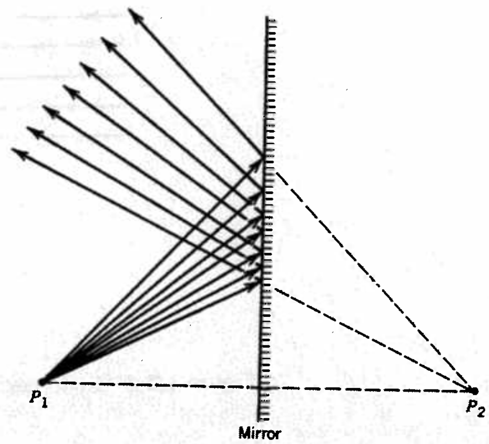

Figure 1.2-1 Reflection from a planar mirror.

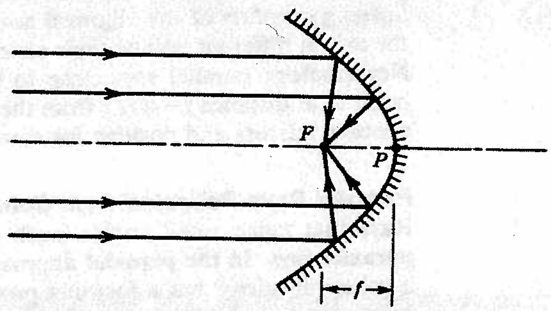

Figure 1.2-2 Focusing of light by a paraboloidal mirror.

mirrors are often used as light-collecting elements in telescopes. They are also used for making parallel beams of light from point sources such as in flashlights.

Elliptical Mirrors

An elliptical mirror reflects all the rays emitted from one of its two foci, e.g., P_1, and images them onto the other focus, P_2 (Fig. 1.2-3). The distances traveled by the light from P_1 to P_2 along any of the paths are all equal, in accordance with Hero's principle.

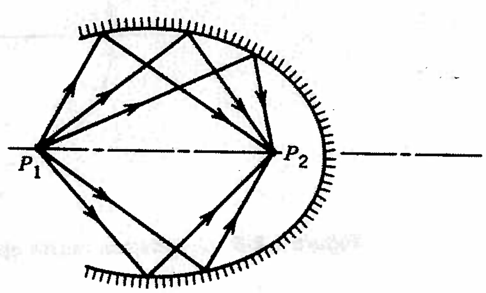

Figure 1.2-3 Reflection from an elliptical mirror.

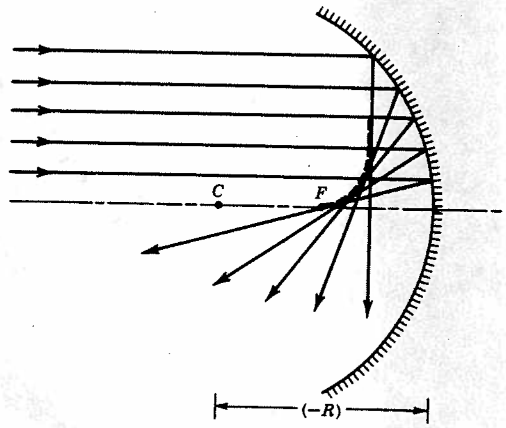

Figure 1.2-4 Reflection of parallel rays from a concave spherical mirror.

Spherical Mirrors

A spherical mirror is easier to fabricate than a paraboloidal or an elliptical mirror. However, it has neither the focusing property of the paraboloidal mirror nor the imaging property of the elliptical mirror. As illustrated in Fig. 1.2-4, parallel rays meet the axis at different points; their envelope (the dashed curve) is called the caustic curve. Nevertheless, parallel rays close to the axis are approximately focused onto a single point F at distance $(-R)/2$ from the mirror center C. By convention, R is negative for concave mirrors and positive for convex mirrors.

Paraxial Rays Reflected from Spherical Mirrors

Rays that make small angles (such that $\sin\theta \approx \theta$) with the mirror's axis are called **paraxial rays**. In the **paraxial approximation**, where only paraxial rays are considered, a spherical mirror has a focusing property like that of the paraboloidal mirror *and* an imaging property like that of the elliptical mirror. The body of rules that results from this approximation forms **paraxial optics**, also called first-order optics or Gaussian optics.

A spherical mirror of radius R therefore acts like a paraboloidal mirror of focal length $f = R/2$. This is in fact plausible since at points near the axis, a parabola can be approximated by a circle with radius equal to the parabola's radius of curvature (Fig. 1.2-5).

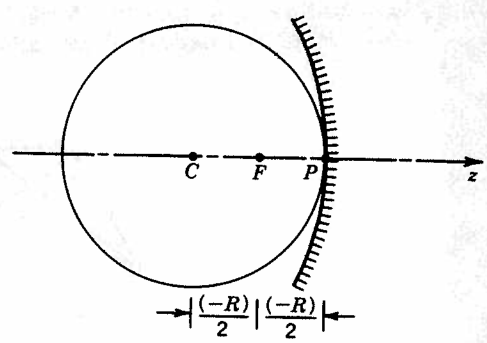

Figure 1.2-5 A spherical mirror approximates a paraboloidal mirror for paraxial rays.

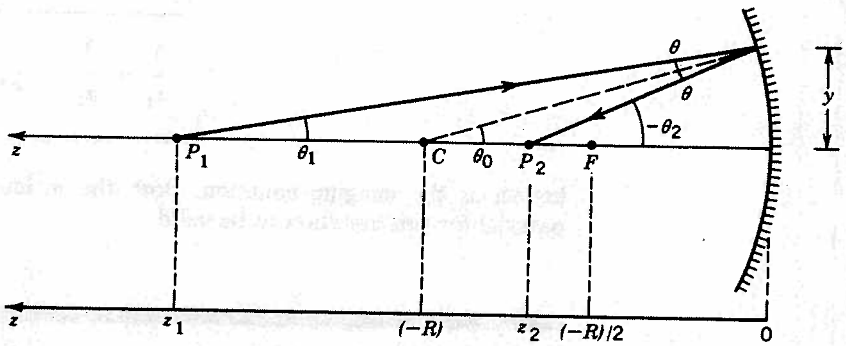

Figure 1.2-6 Reflection of paraxial rays from a concave spherical mirror of radius $R < 0$.

All paraxial rays originating from each point on the axis of a spherical mirror are reflected and focused onto a single corresponding point on the axis. This can be seen (Fig. 1.2-6) by examining a ray emitted at an angle θ_1 from a point P_1 at a distance z_1 away from a concave mirror of radius R, and reflecting at angle $(-\theta_2)$ to meet the axis at a point P_2 a distance z_2 away from the mirror. The angle θ_2 is negative since the ray is traveling downward. Since $\theta_1 = \theta_0 - \theta$ and $(-\theta_2) = \theta_0 + \theta$, it follows that $(-\theta_2) + \theta_1 = 2\theta_0$. If θ_0 is sufficiently small, the approximation $\tan\theta_0 \approx \theta_0$ may be used, so that $\theta_0 \approx y/(-R)$, from which

$$(-\theta_2) + \theta_1 \approx \frac{2y}{-R}, \tag{1.2-1}$$

where y is the height of the point at which the reflection occurs. Recall that R is negative since the mirror is concave. Similarly, if θ_1 and θ_2 are small, $\theta_1 \approx y/z_1$, $(-\theta_2) \approx y/z_2$, and (1.2-1) yields $y/z_1 + y/z_2 \approx 2y/(-R)$, from which

$$\frac{1}{z_1} + \frac{1}{z_2} \approx \frac{2}{-R}. \tag{1.2-2}$$

This relation hold regardless of y (i.e., regardless of θ_1) as long as the approximation is valid. This means that all paraxial rays originating at point P_1 arrive at P_2. The distances z_1 and z_2 are measured in a coordinate system in which the z axis points to the left. Points of negative z therefore lie to the right of the mirror.

According to (1.2-2), rays that are emitted from a point very far out on the z axis ($z_1 = \infty$) are focused to a point F at a distance $z_2 = (-R)/2$. This means that within the paraxial approximation, all rays coming from infinity (parallel to the mirror's axis) are focused to a point at a distance

$$\boxed{f = \frac{-R}{2},} \tag{1.2-3}$$

Focal Length of a Spherical Mirror

which is called the mirror's focal length. Equation (1.2-2) is usually written in the form

$$\frac{1}{z_1} + \frac{1}{z_2} = \frac{1}{f}, \tag{1.2-4}$$

Imaging Equation (Paraxial Rays)

known as the imaging equation. Both the incident and the reflected rays must be paraxial for this equation to be valid.

EXERCISE 1.2-1

Image Formation by a Spherical Mirror. Show that within the paraxial approximation, rays originating from a point $P_1 = (y_1, z_1)$ are reflected to a point $P_2 = (y_2, z_2)$, where z_1 and z_2 satisfy (1.2-4) and $y_2 = -y_1 z_2/z_1$ (Fig. 1.2-7). This means that rays from each point in the plane $z = z_1$ meet at a single corresponding point in the plane $z = z_2$, so that the mirror acts as an image-forming system with magnification $-z_2/z_1$. Negative magnification means that the image is inverted.

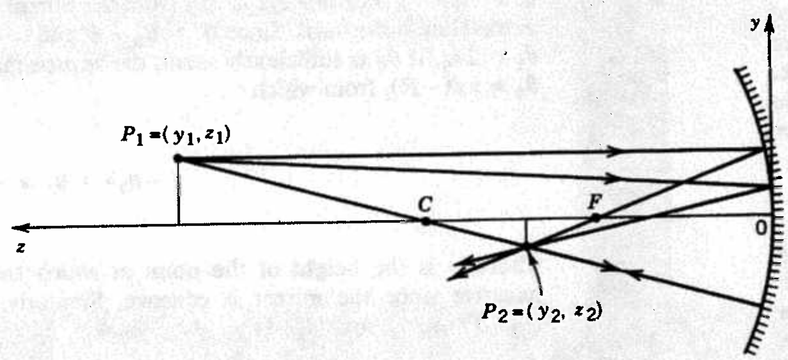

Figure 1.2-7 Image formation by a spherical mirror.

B. Planar Boundaries

The relation between the angles of refraction and incidence, θ_2 and θ_1, at a planar boundary between two media of refractive indices n_1 and n_2 is governed by Snell's law (1.1-1). This relation is plotted in Fig. 1.2-8 for two cases:

- *External Refraction* ($n_1 < n_2$). When the ray is incident from the medium of smaller refractive index, $\theta_2 < \theta_1$ and the refracted ray bends away from the boundary.
- *Internal Refraction* ($n_1 > n_2$). If the incident ray is in a medium of higher refractive index, $\theta_2 > \theta_1$ and the refracted ray bends toward the boundary.

In both cases, when the angles are small (i.e., the rays are paraxial), the relation between θ_2 and θ_1 is approximately linear, $n_1\theta_1 \approx n_2\theta_2$, or $\theta_2 \approx (n_1/n_2)\theta_1$.

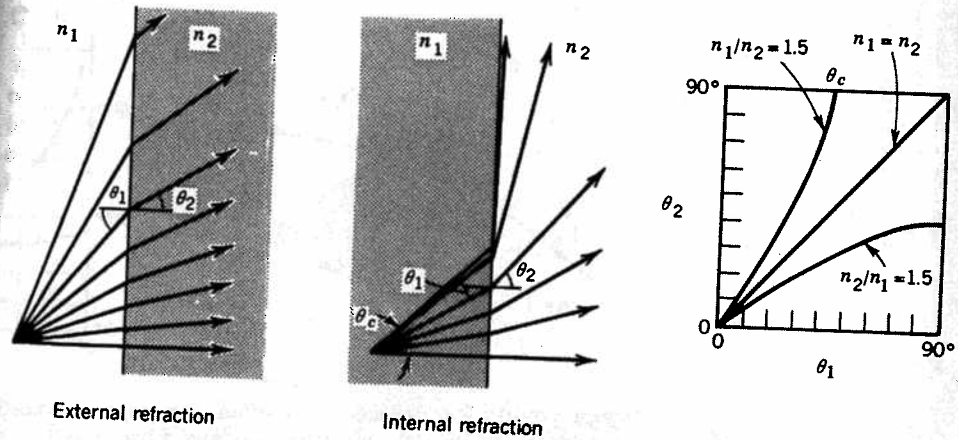

Figure 1.2-8 Relation between the angles of refraction and incidence.

Total Internal Reflection

For internal refraction ($n_1 > n_2$), the angle of refraction is greater than the angle of incidence, $\theta_2 > \theta_1$, so that as θ_1 increases, θ_2 reaches 90° first (see Fig. 1.2-8). This occurs when $\theta_1 = \theta_c$ (the **critical angle**), with $n_1 \sin \theta_c = n_2$, so that

$$\theta_c = \sin^{-1} \frac{n_2}{n_1}. \qquad (1.2\text{-}5)$$

Critical Angle

When $\theta_1 > \theta_c$, Snell's law (1.1-1) cannot be satisfied and refraction does not occur. The incident ray is totally reflected as if the surface were a perfect mirror [Fig. 1.2-9(*a*)]. The phenomenon of total internal reflection is the basis of many optical devices and systems, such as reflecting prisms [see Fig. 1.2-9(*b*)] and optical fibers (see Sec. 1.2D).

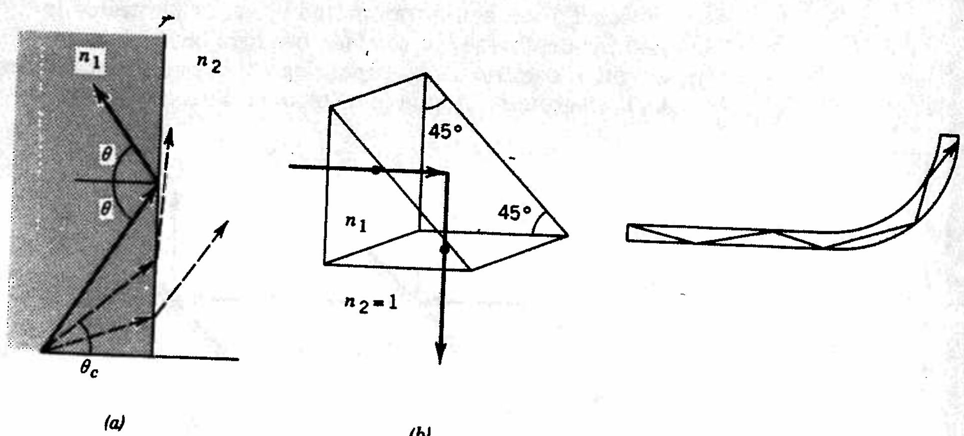

Figure 1.2-9 (*a*) Total internal reflection at a planar boundary. (*b*) The reflecting prism. If $n_1 > \sqrt{2}$ and $n_2 = 1$ (air), then $\theta_c < 45°$; since $\theta_1 = 45°$, the ray is totally reflected. (*c*) Rays are guided by total internal reflection from the internal surface of an optical fiber.

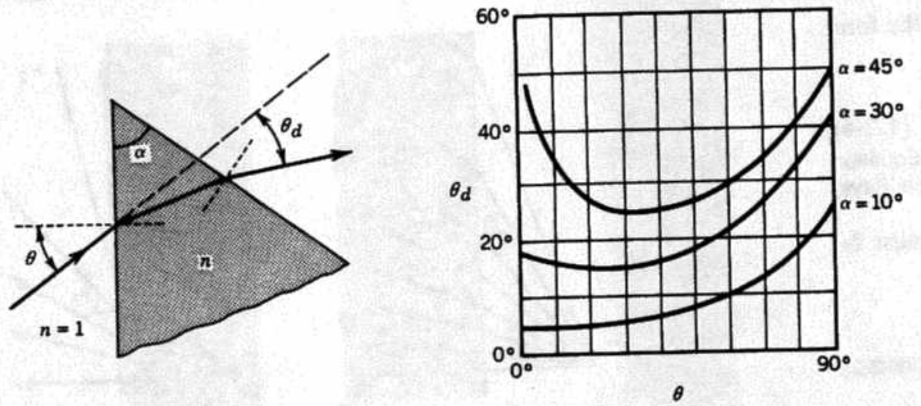

Figure 1.2-10 Ray deflection by a prism. The angle of deflection θ_d as a function of the angle of incidence θ for different apex angles α when $n = 1.5$. When both α and θ are small $\theta_d \approx (n-1)\alpha$, which is approximately independent of θ. When $\alpha = 45°$ and $\theta = 0°$, total internal reflection occurs, as illustrated in Fig. 1.2-9(*b*).

Prisms

A prism of apex angle α and refractive index n (Fig. 1.2-10) deflects a ray incident at an angle θ by an angle

$$\theta_d = \theta - \alpha + \sin^{-1}\left[(n^2 - \sin^2\theta)^{1/2}\sin\alpha - \sin\theta\cos\alpha\right]. \tag{1.2-6}$$

This may be shown by using Snell's law twice at the two refracting surfaces of the prism. When α is very small (thin prism) and θ is also very small (paraxial approximation), (1.2-6) is approximated by

$$\theta_d \approx (n-1)\alpha. \tag{1.2-7}$$

Beamsplitters

The beamsplitter is an optical component that splits the incident light beam into a reflected beam and a transmitted beam, as illustrated in Fig. 1.2-11. Beamsplitters are also frequently used to combine two light beams into one [Fig. 1.2-11(*c*)]. Beamsplitters are often constructed by depositing a thin semitransparent metallic or dielectric film on a glass substrate. A thin glass plate or a prism can also serve as a beamsplitter.

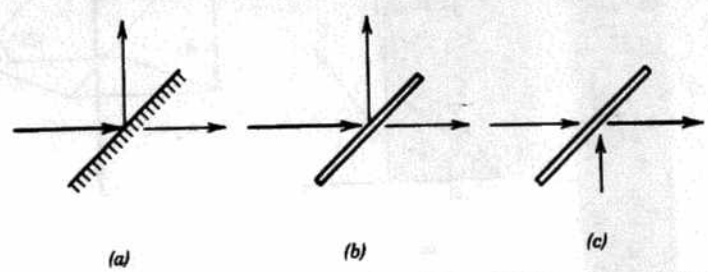

Figure 1.2-11 Beamsplitters and combiners: (*a*) partially reflective mirror; (*b*) thin glass plate; (*c*) beam combiner.

C. Spherical Boundaries and Lenses

We now examine the refraction of rays from a spherical boundary of radius R between two media of refractive indices n_1 and n_2. By convention, R is positive for a convex boundary and negative for a concave boundary. By using Snell's law, and considering only paraxial rays making small angles with the axis of the system so that $\tan\theta \approx \theta$, the following properties may be shown to hold:

- A ray making an angle θ_1 with the z axis and meeting the boundary at a point of height y [see Fig. 1.2-12(*a*)] refracts and changes direction so that the refracted ray makes an angle θ_2 with the z axis,

$$\theta_2 \approx \frac{n_1}{n_2}\theta_1 - \frac{n_2 - n_1}{n_2 R} y. \tag{1.2-8}$$

- All paraxial rays originating from a point $P_1 = (y_1, z_1)$ in the $z = z_1$ plane meet at a point $P_2 = (y_2, z_2)$ in the $z = z_2$ plane, where

$$\frac{n_1}{z_1} + \frac{n_2}{z_2} \approx \frac{n_2 - n_1}{R} \tag{1.2-9}$$

and

$$y_2 = -\frac{z_2}{z_1} y_1. \tag{1.2-10}$$

The $z = z_1$ and $z = z_2$ planes are said to be conjugate planes. Every point in the first plane has a corresponding point (image) in the second with magnification

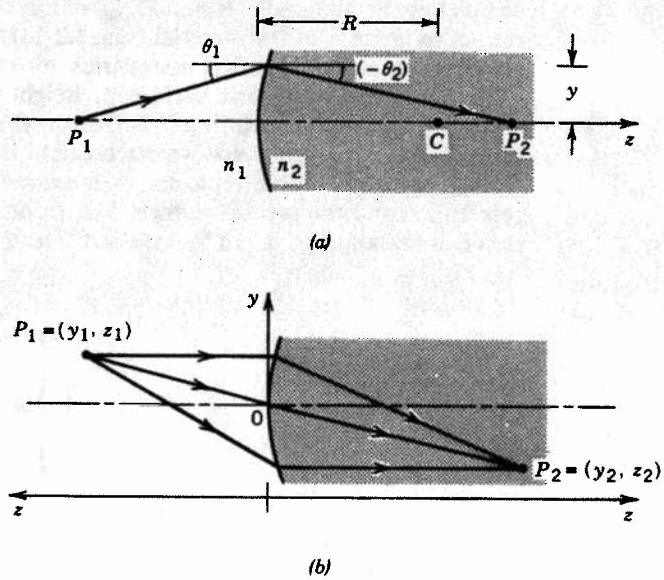

Figure 1.2-12 Refraction at a convex spherical boundary ($R > 0$).

$-z_2/z_1$. Again, negative magnification means that the image is inverted. By convention P_1 is measured in a coordinate system pointing to the left and P_2 in a coordinate system pointing to the right (e.g., if P_2 lies to the left of the boundary, then z_2 would be negative).

The similarities between these properties and those of the spherical mirror are evident. It is important to remember that the image formation properties described above are approximate. They hold only for paraxial rays. Rays of large angles do not obey these paraxial laws; the deviation results in image distortion called **aberration**.

EXERCISE 1.2-2

Image Formation. Derive (1.2-8). Prove that paraxial rays originating from P_1 pass through P_2 when (1.2-9) and (1.2-10) are satisfied.

EXERCISE 1.2-3

Aberration-Free Imaging Surface. Determine the equation of a convex aspherical (nonspherical) surface between media of refractive indices n_1 and n_2 such that all rays (not necessarily paraxial) from an axial point P_1 at a distance z_1 to the left of the surface are imaged onto an axial point P_2 at a distance z_2 to the right of the surface [Fig. 1.2-12(a)]. *Hint:* In accordance with Fermat's principle the optical path lengths between the two points must be equal for all paths.

Lenses

A spherical lens is bounded by two spherical surfaces. It is, therefore, defined completely by the radii R_1 and R_2 of its two surfaces, its thickness Δ, and the refractive index n of the material (Fig. 1.2-13). A glass lens in air can be regarded as a combination of two spherical boundaries, air-to-glass and glass-to-air.

A ray crossing the first surface at height y and angle θ_1 with the z axis [Fig. 1.2-14(a)] is traced by applying (1.2-8) at the first surface to obtain the inclination angle θ of the refracted ray, which we extend until it meets the second surface. We then use (1.2-8) once more with θ replacing θ_1 to obtain the inclination angle θ_2 of the ray after refraction from the second surface. The results are in general complicated. When the lens is thin, however, it can be assumed that the incident ray emerges from the lens at

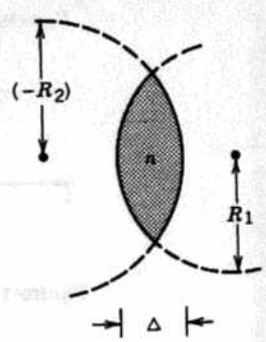

Figure 1.2-13 A biconvex spherical lens.

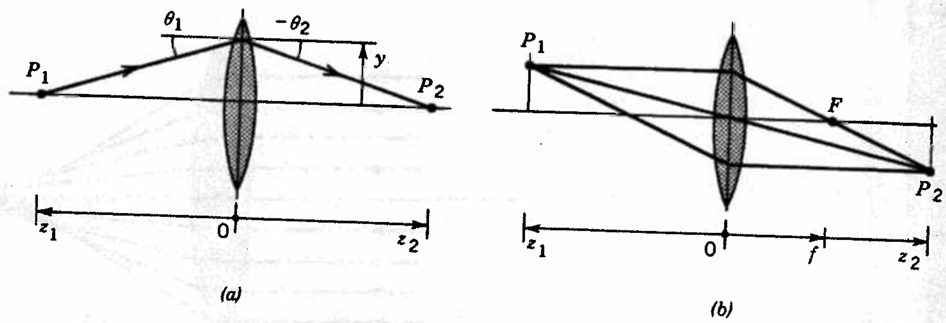

Figure 1.2-14 (*a*) Ray bending by a thin lens. (*b*) Image formation by a thin lens.

about the same height y at which it enters. Under this assumption, the following relations follow:

- The angles of the refracted and incident rays are related by

$$\theta_2 = \theta_1 - \frac{y}{f}, \tag{1.2-11}$$

where f, called the **focal length**, is given by

$$\frac{1}{f} = (n-1)\left(\frac{1}{R_1} - \frac{1}{R_2}\right). \tag{1.2-12}$$

Focal Length of a Thin Spherical Lens

- All rays originating from a point $P_1 = (y_1, z_1)$ meet at a point $P_2 = (y_2, z_2)$ [Fig. 1.2-14(*b*)], where

$$\frac{1}{z_1} + \frac{1}{z_2} = \frac{1}{f} \tag{1.2-13}$$

Imaging Equation

and

$$y_2 = -\frac{z_2}{z_1} y_1. \tag{1.2-14}$$

Magnification

This means that each point in the $z = z_1$ plane is imaged onto a corresponding point in the $z = z_2$ plane with the magnification factor $-z_2/z_1$. The focal length f of a lens therefore completely determines its effect on paraxial rays.

As indicated earlier, P_1 and P_2 are measured in coordinate systems pointing to the left and right, respectively, and the radii of curvatures R_1 and R_2 are positive for convex surfaces and negative for concave surfaces. For the biconvex lens shown in Fig. 1.2-13, R_1 is positive and R_2 is negative, so that the two terms of (1.2-12) add and provide a positive f.

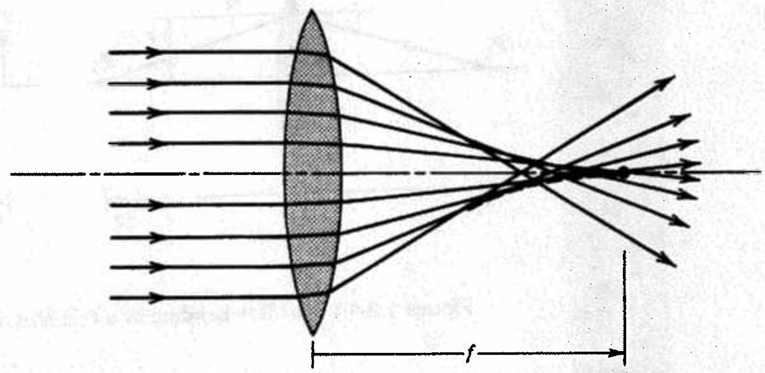

Figure 1.2-15 Nonparaxial rays do not meet at the paraxial focus. The dashed envelope of the refracted rays is called the caustic curve.

EXERCISE 1.2-4

Proof of the Thin Lens Formulas. Using (1.2-8), prove (1.2-11), (1.2-12), and (1.2-13).

It is emphasized once more that the foregoing relations hold only for paraxial rays. The deviations of nonparaxial rays from these relations result in aberrations, as illustrated in Fig. 1.2-15.

D. Light Guides

Light may be guided from one location to another by use of a set of lenses or mirrors, as illustrated schematically in Fig. 1.2-16. Since refractive elements (such as lenses) are usually partially reflective and since mirrors are partially absorptive, the cumulative loss of optical power will be significant when the number of guiding elements is large. Components in which these effects are minimized can be fabricated (e.g., antireflection coated lenses), but the system is generally cumbersome and costly.

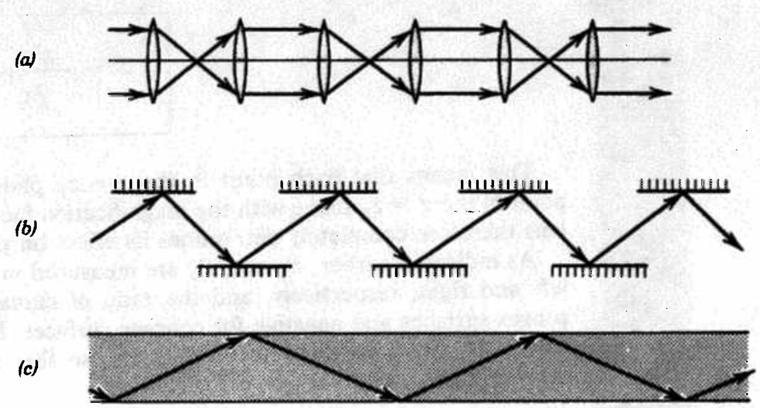

Figure 1.2-16 Guiding light: (*a*) lenses; (*b*) mirrors; (*c*) total internal reflection.

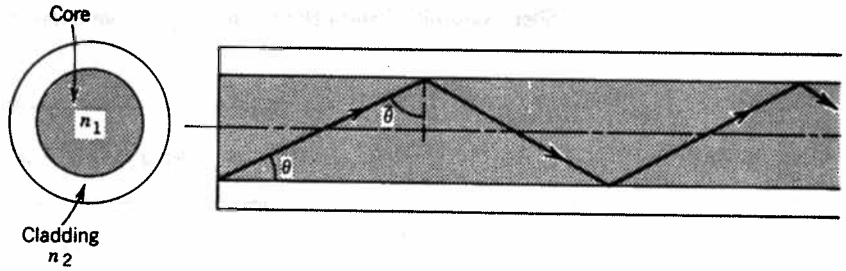

Figure 1.2-17 The optical fiber. Light rays are guided by multiple total internal reflections.

An ideal mechanism for guiding light is that of total internal reflection at the boundary between two media of different refractive indices. Rays are reflected repeatedly without undergoing refraction. Glass fibers of high chemical purity are used to guide light for tens of kilometers with relatively low loss of optical power.

An optical fiber is a light conduit made of two concentric glass (or plastic) cylinders (Fig. 1.2-17). The inner, called the core, has a refractive index n_1, and the outer, called the cladding, has a slightly smaller refractive index, $n_2 < n_1$. Light rays traveling in the core are totally reflected from the cladding if their angle of incidence is greater than the critical angle, $\bar{\theta} > \theta_c = \sin^{-1}(n_2/n_1)$. The rays making an angle $\theta = 90° - \bar{\theta}$ with the optical axis are therefore confined in the fiber core if $\theta < \bar{\theta}_c$, where $\bar{\theta}_c = 90° - \theta_c = \cos^{-1}(n_2/n_1)$. Optical fibers are used in optical communication systems (see Chaps. 8 and 22). Some important properties of optical fibers are derived in Exercise 1.2-5.

Trapping of Light in Media of High Refractive Index

It is often difficult for light originating inside a medium of large refractive index to be extracted into air, especially if the surfaces of the medium are parallel. This occurs since certain rays undergo multiple total internal reflections without ever refracting into air. The principle is illustrated in Exercise 1.2-6.

EXERCISE 1.2-5

Numerical Aperture and Angle of Acceptance of an Optical Fiber. An optical fiber is illuminated by light from a source (e.g., a light-emitting diode, LED). The refractive indices of the core and cladding of the fiber are n_1 and n_2, respectively, and the refractive index of air is 1 (Fig. 1.2-18). Show that the angle θ_a of the cone of rays accepted by the

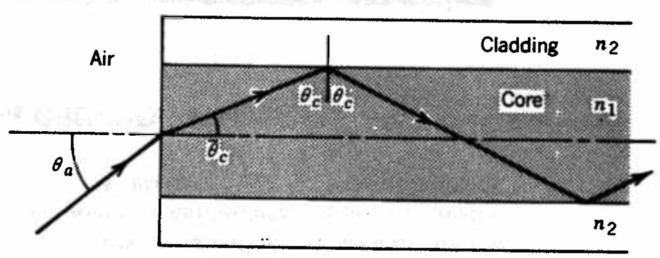

Figure 1.2-18 Acceptance angle of an optical fiber.

fiber (transmitted through the fiber without undergoing refraction at the cladding) is given by

$$\text{NA} = \sin\theta_a = \left(n_1^2 - n_2^2\right)^{1/2}. \tag{1.2-15}$$

Numerical Aperture of an Optical Fiber

The parameter NA $= \sin\theta_a$ is known as the **numerical aperture** of the fiber. Calculate the numerical aperture and acceptance angle for a silica glass fiber with $n_1 = 1.475$ and $n_2 = 1.460$.

EXERCISE 1.2-6

Light Trapped in a Light-Emitting Diode

(a) Assume that light is generated in all directions inside a material of refractive index n cut in the shape of a parallelepiped (Fig. 1.2-19). The material is surrounded by air with refractive index 1. This process occurs in light-emitting diodes (see Chap. 16). What is the angle of the cone of light rays (inside the material) that will emerge from each face? What happens to the other rays? What is the numerical value of this angle for GaAs ($n = 3.6$)?

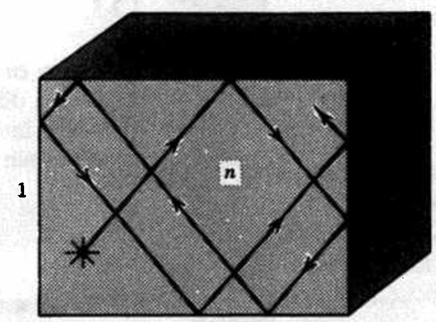

Figure 1.2-19 Trapping of light in a parallelepiped of high refractive index.

(b) Assume that when light is generated isotropically the amount of optical power associated with the rays in a given cone is proportional to the solid angle of the cone. Show that the ratio of the optical power that is extracted from the material to the total generated optical power is $3[1 - (1 - 1/n^2)^{1/2}]$, provided that $n > \sqrt{2}$. What is the numerical value of this ratio for GaAs?

1.3 GRADED-INDEX OPTICS

A graded-index (GRIN) material has a refractive index that varies with position in accordance with a continuous function $n(\mathbf{r})$. These materials are often fabricated by adding impurities (dopants) of controlled concentrations. In a GRIN medium the optical rays follow curved trajectories, instead of straight lines. By appropriate choice of $n(\mathbf{r})$, a GRIN plate can have the same effect on light rays as a conventional optical component, such as a prism or a lens.

A. The Ray Equation

To determine the trajectories of light rays in an inhomogeneous medium with refractive index $n(\mathbf{r})$, we use Fermat's principle,

$$\delta \int_A^B n(\mathbf{r})\, ds = 0,$$

where ds is a differential length along the ray trajectory between A and B. If the trajectory is described by the functions $x(s)$, $y(s)$, and $z(s)$, where s is the length of the trajectory (Fig. 1.3-1), then using the calculus of variations it can be shown† that $x(s)$, $y(s)$, and $z(s)$ must satisfy three partial differential equations,

$$\frac{d}{ds}\left(n\frac{dx}{ds}\right) = \frac{\partial n}{\partial x}, \qquad \frac{d}{ds}\left(n\frac{dy}{ds}\right) = \frac{\partial n}{\partial y}, \qquad \frac{d}{ds}\left(n\frac{dz}{ds}\right) = \frac{\partial n}{\partial z}. \qquad (1.3\text{-}1)$$

By defining the vector $\mathbf{r}(s)$, whose components are $x(s)$, $y(s)$, and $z(s)$, (1.3-1) may be written in the compact vector form

$$\frac{d}{ds}\left(n\frac{d\mathbf{r}}{ds}\right) = \nabla n, \qquad (1.3\text{-}2)$$

Ray Equation

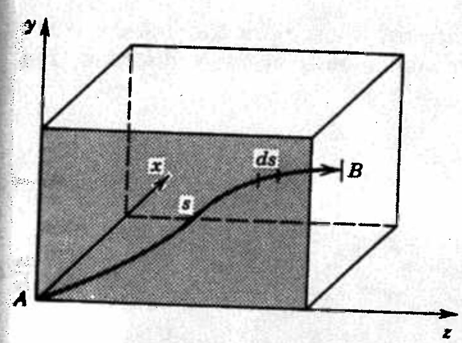

Figure 1.3-1 The ray trajectory is described parametrically by three functions $x(s)$, $y(s)$, and $z(s)$, or by two functions $x(z)$ and $y(z)$.

†This derivation is beyond the scope of this book; see, e.g., R. Weinstock, *Calculus of Variation*, Dover, New York, 1974.

Figure 1.3-2 Trajectory of a paraxial ray in a graded-index medium.

where ∇n, the gradient of n, is a vector with Cartesian components $\partial n/\partial x$, $\partial n/\partial y$, and $\partial n/\partial z$. Equation (1.3-2) is known as the **ray equation**.

One approach to solving the ray equation is to describe the trajectory by two functions $x(z)$ and $y(z)$, write $ds = dz[1 + (dx/dz)^2 + (dy/dz)^2]^{1/2}$, and substitute in (1.3-2) to obtain two partial differential equations for $x(z)$ and $y(z)$. The algebra is generally not trivial, but it simplifies considerably when the paraxial approximation is used.

The Paraxial Ray Equation

In the paraxial approximation, the trajectory is almost parallel to the z axis, so that $ds \approx dz$ (Fig. 1.3-2). The ray equations (1.3-1) then simplify to

$$\frac{d}{dz}\left(n\frac{dx}{dz}\right) \approx \frac{\partial n}{\partial x}, \qquad \frac{d}{dz}\left(n\frac{dy}{dz}\right) \approx \frac{\partial n}{\partial y}. \tag{1.3-3}$$

Paraxial Ray Equations

Given $n = n(x, y, z)$, these two partial differential equations may be solved for the trajectory $x(z)$ and $y(z)$.

In the limiting case of a homogeneous medium for which n is independent of x, y, z, (1.3-3) gives $d^2x/d^2z = 0$ and $d^2y/d^2z = 0$, from which it follows that x and y are linear functions of z, so that the trajectories are straight lines. More interesting cases will be examined subsequently.

B. Graded-Index Optical Components

Graded-Index Slab

Consider a slab of material whose refractive index $n = n(y)$ is uniform in the x and z directions but varies continuously in the y direction (Fig. 1.3-3). The trajectories of

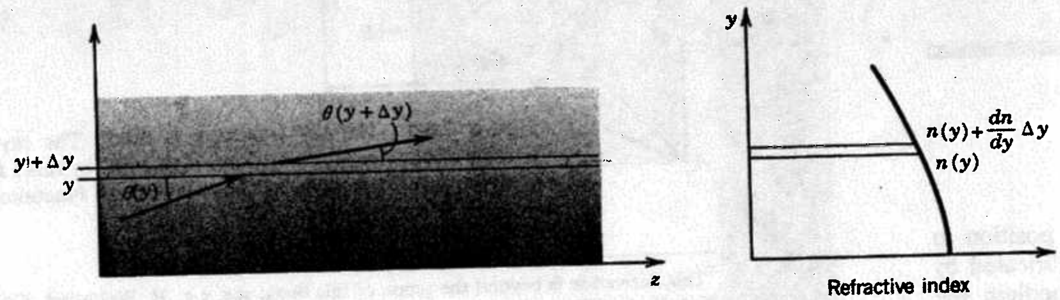

Figure 1.3-3 Refraction in a graded-index slab.

paraxial rays in the y–z plane are described by the paraxial ray equation

$$\frac{d}{dz}\left(n\frac{dy}{dz}\right) = \frac{dn}{dy}, \qquad (1.3\text{-}4)$$

from which

$$\frac{d^2y}{dz^2} = \frac{1}{n}\frac{dn}{dy}. \qquad (1.3\text{-}5)$$

Given $n(y)$ and the initial conditions (y and dy/dz at $z = 0$), (1.3-5) can be solved for the function $y(z)$, which describes the ray trajectories.

Derivation of the Paraxial Ray Equation in a Graded-Index Slab Using Snell's Law

Equation (1.3-5) may also be derived by the direct use of Snell's law (Fig. 1.3-3). Let $\theta(y) \approx dy/dz$ be the angle that the ray makes with the z-axis at the position (y, z). After traveling through a layer of width Δy the ray changes its angle to $\theta(y + \Delta y)$. The two angles are related by Snell's law,

$$n(y)\cos\theta(y) = n(y + \Delta y)\cos\theta(y + \Delta y)$$

$$= \left[n(y) + \frac{dn}{dy}\Delta y\right]\left[\cos\theta(y) - \frac{d\theta}{dy}\Delta y \sin\theta(y)\right],$$

where we have applied the expansion $f(y + \Delta y) = f(y) + (df/dy)\,\Delta y$ to the function $f(y) = \cos\theta(y)$. In the limit $\Delta y \to 0$, we obtain the differential equation

$$\frac{dn}{dy} = n\tan\theta\frac{d\theta}{dy}. \qquad (1.3\text{-}6)$$

For paraxial rays θ is very small so that $\tan\theta \approx \theta$. Substituting $\theta = dy/dz$ in (1.3-6), we obtain (1.3-5).

EXAMPLE 1.3-1. ***Slab with Parabolic Index Profile.*** An important particular distribution for the graded refractive index is

$$n^2(y) = n_0^2(1 - \alpha^2 y^2). \qquad (1.3\text{-}7)$$

This is a symmetric function of y that has its maximum value at $y = 0$ (Fig. 1.3-4). A glass slab with this profile is known by the trade name SELFOC. Usually, α is chosen to be sufficiently small so that $\alpha^2 y^2 \ll 1$ for all y of interest. Under this condition, $n(y) = n_0(1 - \alpha^2 y^2)^{1/2} \approx n_0(1 - \frac{1}{2}\alpha^2 y^2)$; i.e., $n(y)$ is a parabolic distribution. Also, because

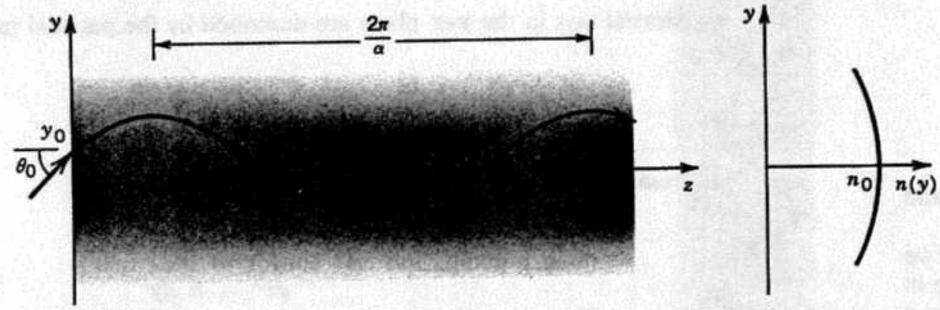

Figure 1.3-4 Trajectory of a ray in a GRIN slab of parabolic index profile (SELFOC).

$n(y) - n_0 \ll n_0$, the fractional change of the refractive index is very small. Taking the derivative of (1.3-7), the right-hand side of (1.3-5) is $(1/n)\,dn/dy = -(n_0/n)^2\alpha^2 y \approx -\alpha^2 y$, so that (1.3-5) becomes

$$\frac{d^2y}{dz^2} \approx -\alpha^2 y. \tag{1.3-8}$$

The solutions of this equation are harmonic functions with period $2\pi/\alpha$. Assuming an initial position $y(0) = y_0$ and an initial slope $dy/dz = \theta_0$ at $z = 0$,

$$y(z) = y_0 \cos \alpha z + \frac{\theta_0}{\alpha} \sin \alpha z, \tag{1.3-9}$$

from which the slope of the trajectory is

$$\theta(z) = \frac{dy}{dz} = -y_0\alpha \sin \alpha z + \theta_0 \cos \alpha z. \tag{1.3-10}$$

The ray oscillates about the center of the slab with a period $2\pi/\alpha$ known as the **pitch**, as illustrated in Fig. 1.3-4.

The maximum excursion of the ray is $y_{max} = [y_0^2 + (\theta_0/\alpha)^2]^{1/2}$ and the maximum angle is $\theta_{max} = \alpha y_{max}$. The validity of this approximate analysis is ensured if $\theta_{max} \ll 1$. If $2y_{max}$ is smaller than the width of the slab, the ray remains confined and the slab serves as a light guide. Figure 1.3-5 shows the trajectories of a number of rays transmitted through a SELFOC slab. Note that all rays have the same pitch. This GRIN slab may be used as a lens, as demonstrated in Exercise 1.3-1.

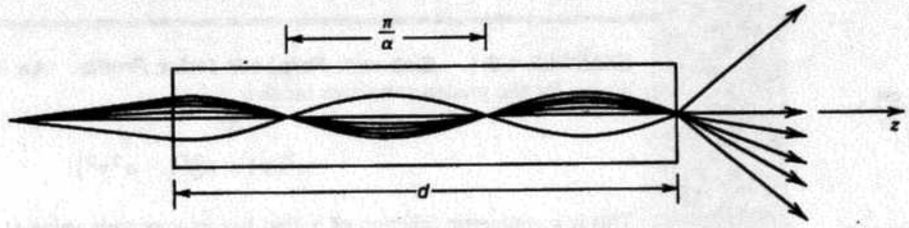

Figure 1.3-5 Trajectories of rays in a SELFOC slab.

EXERCISE 1.3-1

The GRIN Slab as a Lens. Show that a SELFOC slab of length $d < \pi/2\alpha$ and refractive index given by (1.3-7) acts as a cylindrical lens (a lens with focusing power in the y-z plane) of focal length

$$f \approx \frac{1}{n_0 \alpha \sin \alpha d}. \tag{1.3-11}$$

Show that the principal point (defined in Fig. 1.3-6) lies at a distance from the slab edge $\overline{AH} \approx (1/n_0\alpha)\tan(\alpha d/2)$. Sketch the ray trajectories in the special cases $d = \pi/\alpha$ and $\pi/2\alpha$.

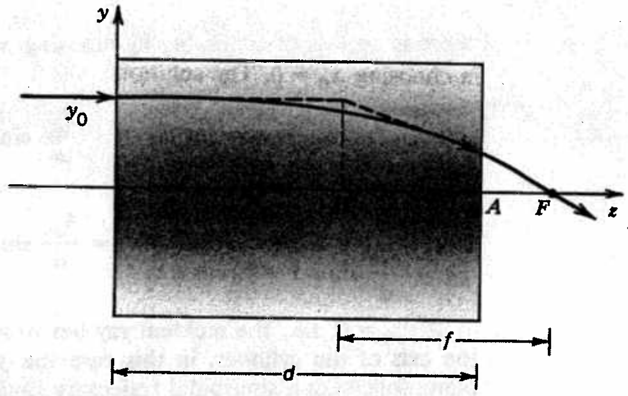

Figure 1.3-6 The SELFOC slab used as a lens; F is the focal point and H is the principal point.

Graded-Index Fibers

A graded-index fiber is a glass cylinder with a refractive index n that varies as a function of the radial distance from its axis. In the paraxial approximation, the ray trajectories are governed by the paraxial ray equations (1.3-3). Consider, for example, the distribution

$$n^2 = n_0^2\left[1 - \alpha^2(x^2 + y^2)\right]. \tag{1.3-12}$$

Substituting (1.3-12) into (1.3-3) and assuming that $\alpha^2(x^2 + y^2) \ll 1$ for all x and y of interest, we obtain

$$\frac{d^2x}{dz^2} \approx -\alpha^2 x, \qquad \frac{d^2y}{dz^2} \approx -\alpha^2 y. \tag{1.3-13}$$

Both x and y are therefore harmonic functions of z with period $2\pi/\alpha$. The initial positions (x_0, y_0) and angles $(\theta_{x0} = dx/dz$ and $\theta_{y0} = dy/dz)$ at $z = 0$ determine the amplitudes and phases of these harmonic functions. Because of the circular symmetry,

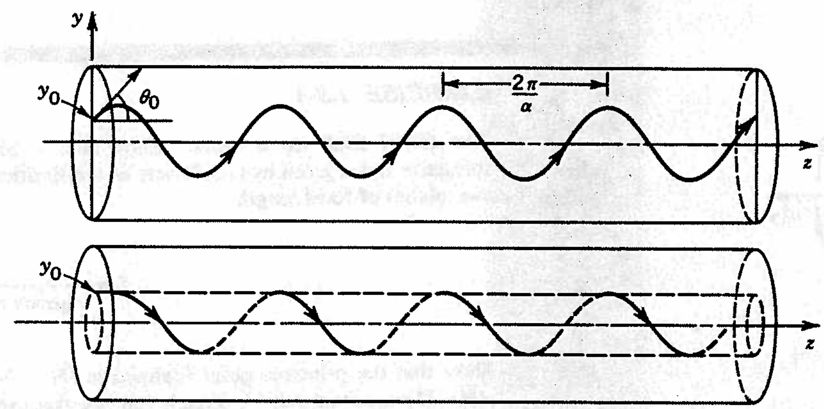

Figure 1.3-7 (*a*) Meridional and (*b*) helical rays in a graded-index fiber with parabolic index profile.

there is no loss of generality in choosing $x_0 = 0$. The solution of (1.3-13) is then

$$x(z) = \frac{\theta_{x0}}{\alpha} \sin \alpha z$$
$$y(z) = \frac{\theta_{y0}}{\alpha} \sin \alpha z + y_0 \cos \alpha z. \tag{1.3-14}$$

If $\theta_{x0} = 0$, i.e., the incident ray lies in a meridional plane (a plane passing through the axis of the cylinder, in this case the y–z plane), the ray continues to lie in that plane following a sinusoidal trajectory similar to that in the GRIN slab [Fig. 1.3-7(*a*)].

On the other hand, if $\theta_{y0} = 0$, and $\theta_{x0} = \alpha y_0$, then

$$x(z) = y_0 \sin \alpha z$$
$$y(z) = y_0 \cos \alpha z, \tag{1.3-15}$$

so that the ray follows a helical trajectory lying on the surface of a cylinder of radius y_0 [Fig. 1.3-7(*b*)]. In both cases the ray remains confined within the fiber, so that the fiber serves as a light guide. Other helical patterns are generated with different incident rays.

Graded-index fibers and their use in optical communications are discussed in Chaps. 8 and 22.

EXERCISE 1.3-2

Numerical Aperture of the Graded-Index Fiber. Consider a graded-index fiber with the index profile in (1.3-12) and radius a. A ray is incident from air into the fiber at its center, making an angle θ_0 with the fiber axis (see Fig. 1.3-8). Show, in the paraxial

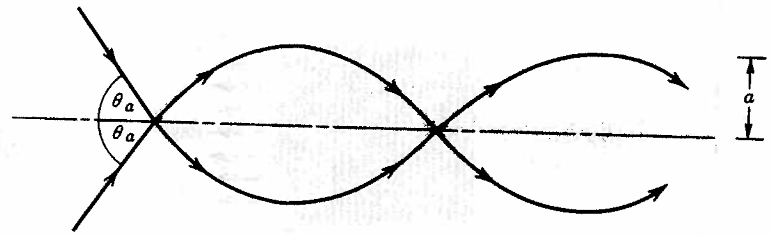

Figure 1.3-8 Acceptance angle of a graded-index optical fiber.

approximation, that the numerical aperture is

$$\boxed{\text{NA} = \sin\theta_a \approx n_0 a\alpha,}$$

(1.3-16)
Numerical Aperture
(Graded-Index Fiber)

where θ_a is the maximum angle θ_0 for which the ray trajectory is confined within the fiber. Compare this to the numerical aperture of a step-index fiber such as the one discussed in Exercise 1.2-5. To make the comparison fair, take the refractive indices of the core and cladding of the step-index fiber to be $n_1 = n_0$ and $n_2 = n_0(1 - \alpha^2 a^2)^{1/2} \approx n_0(1 - \frac{1}{2}\alpha^2 a^2)$.

*C. The Eikonal Equation

The ray trajectories are often characterized by the surfaces to which they are normal. Let $S(\mathbf{r})$ be a scalar function such that its equilevel surfaces, $S(\mathbf{r})$ = constant, are everywhere normal to the rays (Fig. 1.3-9). If $S(\mathbf{r})$ is known, the ray trajectories can readily be constructed since the normal to the equilevel surfaces at a position $\mathbf{r}$ is in the direction of the gradient vector $\nabla S(\mathbf{r})$. The function $S(\mathbf{r})$, called the **eikonal**, is akin to the potential function $V(\mathbf{r})$ in electrostatics; the role of the optical rays is played by the lines of electric field $\mathbf{E} = -\nabla V$.

To satisfy Fermat's principle (which is the main postulate of ray optics) the eikonal $S(\mathbf{r})$ must satisfy a partial differential equation known as the **eikonal equation**,

$$\left(\frac{\partial S}{\partial x}\right)^2 + \left(\frac{\partial S}{\partial y}\right)^2 + \left(\frac{\partial S}{\partial z}\right)^2 = n^2, \tag{1.3-17}$$

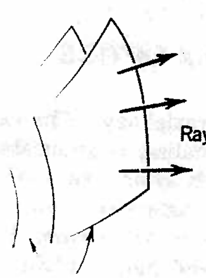

Figure 1.3-9 Ray trajectories are normal to the surfaces of constant $S(\mathbf{r})$.

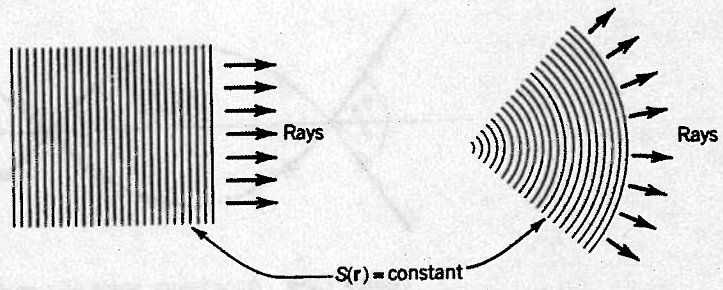

Figure 1.3-10 Rays and surfaces of constant $S(\mathbf{r})$ in a homogeneous medium.

which is usually written in the vector form

$$|\nabla S|^2 = n^2, \tag{1.3-18}$$

Eikonal Equation

where $|\nabla S|^2 = \nabla S \cdot \nabla S$. The proof of the eikonal equation from Fermat's principle is a mathematical exercise that lies beyond the scope of this book.† Fermat's principle (and the ray equation) can also be shown to follow from the eikonal equation. Therefore, either the eikonal equation or Fermat's principle may be regarded as the principal postulate of ray optics.

Integrating the eikonal equation (1.3-18) along a ray trajectory between two points A and B gives

$$S(\mathbf{r}_B) - S(\mathbf{r}_A) = \int_A^B |\nabla S|\, ds = \int_A^B n\, ds = \text{optical path length between } A \text{ and } B.$$

This means that the difference $S(\mathbf{r}_B) - S(\mathbf{r}_A)$ represents the optical path length between A and B. In the electrostatics analogy, the optical path length plays the role of the potential difference.

To determine the ray trajectories in an inhomogeneous medium of refractive index $n(\mathbf{r})$, we can either solve the ray equation (1.3-2), as we have done earlier, or solve the eikonal equation for $S(\mathbf{r})$, from which we calculate the gradient ∇S.

If the medium is homogeneous, i.e., $n(\mathbf{r})$ is constant, the magnitude of ∇S is constant, so that the wavefront normals (rays) must be straight lines. The surfaces $S(\mathbf{r}) = \text{constant}$ may be parallel planes or concentric spheres, as illustrated in Fig. 1.3-10.

1.4 MATRIX OPTICS

Matrix optics is a technique for tracing paraxial rays. The rays are assumed to travel only within a single plane, so that the formalism is applicable to systems with planar geometry and to meridional rays in circularly symmetric systems.

A ray is described by its position and its angle with respect to the optical axis. These variables are altered as the ray travels through the system. In the paraxial approximation, the position and angle at the input and output planes of an optical system are

†See, e.g., M. Born and E. Wolf, *Principles of Optics*, Pergamon Press, New York, 6th ed. 1980.

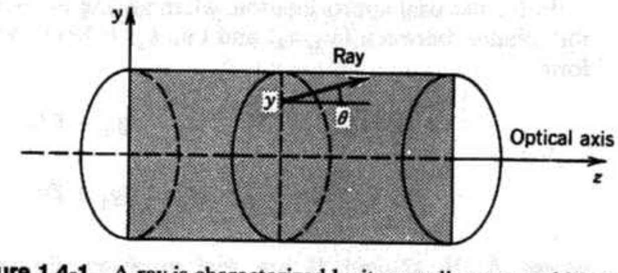

Figure 1.4-1 A ray is characterized by its coordinate y and its angle θ.

related by two *linear* algebraic equations. As a result, the optical system is described by a 2×2 matrix called the ray-transfer matrix.

The convenience of using matrix methods lies in the fact that the ray-transfer matrix of a cascade of optical components (or systems) is a product of the ray-transfer matrices of the individual components (or systems). Matrix optics therefore provides a formal mechanism for describing complex optical systems in the paraxial approximation.

A. The Ray-Transfer Matrix

Consider a circularly symmetric optical system formed by a succession of refracting and reflecting surfaces all centered about the same axis (optical axis). The z axis lies along the optical axis and points in the general direction in which the rays travel. Consider rays in a plane containing the optical axis, say the y–z plane. We proceed to trace a ray as it travels through the system, i.e., as it crosses the transverse planes at different axial distances. A ray crossing the transverse plane at z is completely characterized by the coordinate y of its crossing point and the angle θ (Fig. 1.4-1).

An optical system is a set of optical components placed between two transverse planes at z_1 and z_2, referred to as the input and output planes, respectively. The system is characterized completely by its effect on an incoming ray of arbitrary position and direction (y_1, θ_1). It steers the ray so that it has new position and direction (y_2, θ_2) at the output plane (Fig. 1.4-2).

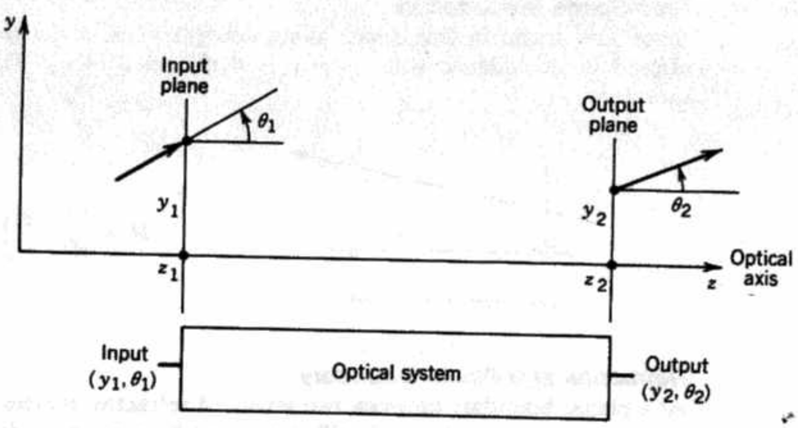

Figure 1.4-2 A ray enters an optical system at position y_1 and angle θ_1 and leaves at position y_2 and angle θ_2.

In the paraxial approximation, when all angles are sufficiently small so that $\sin\theta \approx \theta$, the relation between (y_2, θ_2) and (y_1, θ_1) is linear and can generally be written in the form

$$y_2 = Ay_1 + B\theta_1 \tag{1.4-1}$$

$$\theta_2 = Cy_1 + D\theta_1, \tag{1.4-2}$$

where A, B, C and D are real numbers. Equations (1.4-1) and (1.4-2) may be conveniently written in matrix form as

$$\begin{bmatrix} y_2 \\ \theta_2 \end{bmatrix} = \begin{bmatrix} A & B \\ C & D \end{bmatrix} \begin{bmatrix} y_1 \\ \theta_1 \end{bmatrix}.$$

The matrix **M**, whose elements are A, B, C, D, characterizes the optical system completely since it permits (y_2, θ_2) to be determined for any (y_1, θ_1). It is known as the **ray-transfer matrix**.

EXERCISE 1.4-1

Special Forms of the Ray-Transfer Matrix. Consider the following situations in which one of the four elements of the ray-transfer matrix vanishes:

(a) Show that if $A = 0$, all rays that enter the system at the same angle leave at the same position, so that parallel rays in the input are focused to a single point at the output.

(b) What are the special features of each of the systems for which $B = 0$, $C = 0$, or $D = 0$?

B. Matrices of Simple Optical Components

Free-Space Propagation

Since rays travel in free space along straight lines, a ray traversing a distance d is altered in accordance with $y_2 = y_1 + \theta_1 d$ and $\theta_2 = \theta_1$. The ray-transfer matrix is therefore

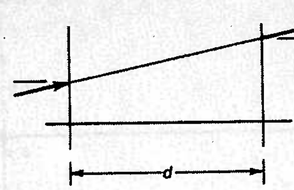

$$\mathbf{M} = \begin{bmatrix} 1 & d \\ 0 & 1 \end{bmatrix}. \tag{1.4-3}$$

Refraction at a Planar Boundary

At a planar boundary between two media of refractive indices n_1 and n_2, the ray angle changes in accordance with Snell's law $n_1 \sin\theta_1 = n_2 \sin\theta_2$. In the paraxial approximation, $n_1\theta_1 \approx n_2\theta_2$. The position of the ray is not altered, $y_2 = y_1$. The ray-transfer matrix is

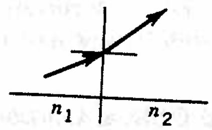

$$\mathbf{M} = \begin{bmatrix} 1 & 0 \\ 0 & \frac{n_1}{n_2} \end{bmatrix}. \qquad (1.4\text{-}4)$$

Refraction at a Spherical Boundary

The relation between θ_1 and θ_2 for paraxial rays refracted at a spherical boundary between two media is provided in (1.2-8). The ray height is not altered, $y_2 \approx y_1$. The ray-transfer matrix is

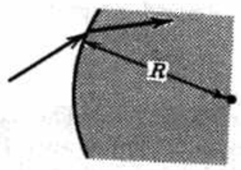

Convex, $R > 0$; concave, $R < 0$

$$\mathbf{M} = \begin{bmatrix} 1 & 0 \\ -\frac{(n_2 - n_1)}{n_2 R} & \frac{n_1}{n_2} \end{bmatrix}. \qquad (1.4\text{-}5)$$

Transmission Through a Thin Lens

The relation between θ_1 and θ_2 for paraxial rays transmitted through a thin lens of focal length f is given in (1.2-11). Since the height remains unchanged ($y_2 = y_1$),

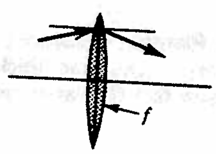

Convex, $f > 0$; concave, $f < 0$

$$\mathbf{M} = \begin{bmatrix} 1 & 0 \\ -\frac{1}{f} & 1 \end{bmatrix}. \qquad (1.4\text{-}6)$$

Reflection from a Planar Mirror

Upon reflection from a planar mirror, the ray position is not altered, $y_2 = y_1$. Adopting the convention that the z axis points in the general direction of travel of the rays, i.e., toward the mirror for the incident rays and away from it for the reflected rays, we conclude that $\theta_2 = \theta_1$. The ray-transfer matrix is therefore the identity matrix

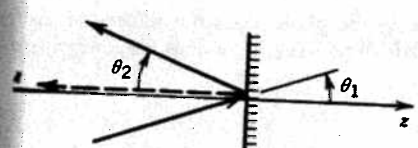

$$\mathbf{M} = \begin{bmatrix} 1 & 0 \\ 0 & 1 \end{bmatrix}. \qquad (1.4\text{-}7)$$

Reflection from a Spherical Mirror

Using (1.2-1), and the convention that the z axis follows the general direction of the rays as they reflect from mirrors, we similarly obtain

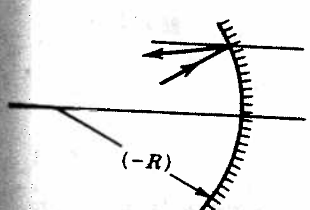

Concave, $R < 0$; convex, $R > 0$

$$\mathbf{M} = \begin{bmatrix} 1 & 0 \\ \frac{2}{R} & 1 \end{bmatrix}. \qquad (1.4\text{-}8)$$

Note the similarity between the ray-transfer matrices of a spherical mirror (1.4-8) and a thin lens (1.4-6). A mirror with radius of curvature R bends rays in a manner that is identical to that of a thin lens with focal length $f = -R/2$.

C. Matrices of Cascaded Optical Components

A cascade of optical components whose ray-transfer matrices are $\mathbf{M}_1, \mathbf{M}_2, \ldots, \mathbf{M}_N$ is equivalent to a single optical component of ray-transfer matrix

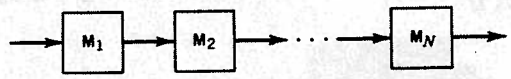

$$\mathbf{M} = \mathbf{M}_N \cdots \mathbf{M}_2 \mathbf{M}_1. \tag{1.4-9}$$

Note the order of matrix multiplication: The matrix of the system that is crossed by the rays first is placed to the right, so that it operates on the column matrix of the incident ray first.

EXERCISE 1.4-2

A Set of Parallel Transparent Plates. Consider a set of N parallel planar transparent plates of refractive indices $n_1, n_2, \ldots, n_N$ and thicknesses $d_1, d_2, \ldots, d_N$, placed in air ($n = 1$) normal to the z axis. Show that the ray-transfer matrix is

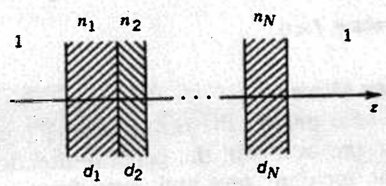

$$\mathbf{M} = \begin{bmatrix} 1 & \displaystyle\sum_{i=1}^{N} \frac{d_i}{n_i} \\ 0 & 1 \end{bmatrix}. \tag{1.4-10}$$

Note that the order of placing the plates does not affect the overall ray-transfer matrix. What is the ray-transfer matrix of an inhomogeneous transparent plate of thickness d_0 and refractive index $n(z)$?

EXERCISE 1.4-3

A Gap Followed by a Thin Lens. Show that the ray-transfer matrix of a distance d of free space followed by a lens of focal length f is

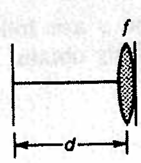

$$\mathbf{M} = \begin{bmatrix} 1 & d \\ -\frac{1}{f} & 1 - \frac{d}{f} \end{bmatrix}. \tag{1.4-11}$$

EXERCISE 1.4-4

Imaging with a Thin Lens. Derive an expression for the ray-transfer matrix of a system comprised of free space/thin lens/free space, as shown in Fig. 1.4-3. Show that if the